Ex vivo Inducing Apoptotic Mesenchymal Stem Cell by High Hydrostatic Pressure

Tien Minh Le
Kansai Ika Daigaku
Naoki Morimoto (mnaoki22@kuhp.kyoto-u.ac.jp)
Kyoto Daigaku https://orcid.org/0000-0002-0712-3172
Nhung Thi My Ly
Kansai Ika Daigaku
Toshihito Mitsui
Kansai Ika Daigaku
Sharon Claudia Notodihardjo
Kansai Ika Daigaku
Natsuko Kakudo
Kansai Ika Daigaku
Kenji Kusumoto
Kansai Ika Daigaku

Research

Keywords: apoptosis, extracellular vesicles, mesenchymal stem cell (MSC), high hydrostatic pressure (HHP), tissue engineering

Posted Date: June 22nd, 2020

DOI: https://doi.org/10.21203/rs.3.rs-36051/v1

Abstract

Background: Apoptosis was reported to take crucial role in mesenchymal stem cell (MSC)-mediated immunomodulation, in which apoptotic MSCs were shown to be superior compared to living MSCs. Furthermore, extracellular vesicles (Evs) derived from MSCs were revealed more specific advantages for patient safety such as lower propensity to trigger innate and adaptive immune responses. As a safety and simple operation, high hydrostatic pressure (HHP), a physical technique that uses only fluid pressure to inactivate cells or tissues, has been developed and applied in a lot of field of biosciences, including biotechnology, biomaterials, or tissue engineering.

Methods: MSCs isolated from human bone marrow were suspended cultured in appropriate medium and subjected to pressurization at 50 MPa for 36 h. Then cells were collected and investigated apoptotic pathway by transmission electron microscopy (TEM), phosphatidylserine membrane translocations, cleaved caspase-3/7 and terminal deoxy-nucleotidyl transferase dUTP nick-end labeling (TUNEL) staining. Besides, viability assays and live cell imaging were also used for assessement of cell survival after pressurization.

Results: We found that HHP at 50 MPa for ≥36 h completely induced MSC death by Live/Dead assay, live cell imaging and WST-8 assay up to 7 days after pressurization. The large amount of apoptotic MSCs death was found based on morphological changes in TEM, phosphatidylserine exposure, caspase activation and detection of DNA fragmentations via TUNEL staining.

Conclusions: In the current study, our data revealed that HHP treatment was convenient processing which safety and effectively induced MSCs undergo apoptosis. Especially, by capable of manufacture expanding, this technique might provide numbers of manipulated products using for industrial cell-based therapies.

Background

Mesenchymal stem/stroma cells (MSCs, a term first coined by Caplan) are nonhematopoietic stem cells derived from bone marrow [1] and have multipotent differentiation capacity to mesodermal tissues, such as bone, tendon, cartilage, muscle, and fat [2]. That finding was expected to open the era of replacing or repairing damaged tissues of mesenchymal origin. Since then, MSCs have received center-stage attention for their broad-ranging clinical potential, and as a focus point in the rapidly growing field of regenerative medicine. Over the past decade, numerous advances have been made in the development of MSCs as a therapy for a highly diverse group of diseases, including cardiac, neural, and orthopedic diseases [3]. In most clinical and pre-clinical models, MSCs were administered intravenously, as this has proven to be safe and allow the administration of large amounts of cells [4]. However, translation of that therapy to the clinical setting has been unclear. The clinical trials have often been controversial with only 40-50% of patients treated by MSCs was effect [3]. There are evidences that after intravenous infusion, the majority of MSCs were trapped in the microvascular network of the lungs and tissues due to their large size [5],

then shortly phagocytosed by blood-derived monocytes and neutrophils there [6]. Recently, Galleu et al. have shown that infused living MSCs are subject to perforin-induced apoptosis through recipient cytotoxic cells. As the cytotoxic cell-induced apoptosis of MSCs was described to be essential for the MSC-mediated immunomodulation, the allogenic components might be the secondary importance [7]. These findings emphasize the importance of apoptosis in MSC-mediated immunomodulation and might explain previous study results, in which apoptotic MSCs (apoMSCs) were shown to be superior compared to living MSCs [8-10]. Besides, numerous studies recently revealed that apoptotic cells release not only apoptotic bodies but also a range of extracellular vesicles (Evs) that can act as biological modulators. They can comprise microvesicles (MVs), including those bearing mitochondria, as well as exosomes that are now recognized as powerful mediators of intercellular communication locally and systemically [11, 12]. One advantage of MVs compared with living cells is their nanoscale size may effectively and functionally cross biological barriers, unlike synthetic drug nanocarriers and whole cells [13].

Furthermore, previous studies have suggested that viable MSCs could favor tumor growth in vivo [14, 15]. The mechanism behind MSC-induced tumor growth involves the formation of carcinoma associated fibroblasts (CAFs). CAFs and CAF-like MSCs produce growth factors, cytokines, and chemokines, and thereby provide the microvascularization and the stromal network for tumor progression [16-18]. As dead MSCs have no active cell metabolism, it can be assumed that they do not differentiate into CAF-like cells with the corresponding secretion of growth factors, cytokines, and chemokines [6, 10]. Notably, dead MSCs may still provoke changes in the tumor microenvironment due to their immunomodulatory properties [19, 20]. Therefore, it is considered that dead or apoptotic MSCs may be an important material of further investigation and development for new approach in the future of cell-based therapies [7, 21]. Along with that, it also requires a new effective method for inducing apoptotic MSCs with the posibilities of widely manufacture.

HHP is a physical technique that uses only fluid pressure in order to inactivate cells or tissues without using any chemical reagents [22, 23]. As its safety and simple operation, HHP nowadays was developed and applied in a lot of field of biosciences, including biotechnology, biomaterials, or tissue engineering [24-26]. While development of that technique, we succeced to completely induce apoptosis of human dermal fibroblasts and skin tissue by persistent HHP exposure at 50 MPa for around 36 hours. Then, in *in vivo* transplantation, the apoptotic skin was shown superior of wound healing and regeneration than conventional method (Le et al., unpublished). We considered that method might have effect for *ex vivo* inducing apoptosis of MSCs and contribute to progression of apoMSC studies in clinical trials. Therefore, in this study, we explored the possibility of inducing human bone marrow-derived MSC apoptosis by using hydrostatic pressure.

Methods

Bone marrow-MSCs identifications and culture

MSCs were derived from human bone marrow and kindly supplied from Japan Tissue Engineering company (Lot No. BKXH-1-P5-79,80; J-TEC, Japan Tissue Engineering Co., Ltd., Gamagori, Aichi, Japan). After rapidly thawing at 37^{o} C water bath, 2×10^{6} cells per cryovial were seeded and cultured on 4 x 10-cm dish (Falcon; Corning Inc., Corning, NY, USA) with BMP01(-) culture medium comprising of aMEM, 15% FBS, and 0.05% Gentamicin (Lot No. 190306; J-TEC Co., Ltd.). Those cells were then incubated in 37^{o} C, 5% CO_2, normoxic incubator and presented fibroblast-like morphology as shown in Figure 1. The medium was changed every 2-3 days and MSCs were subcultured when reached 80-90% confluent. MSCs at passages 6-10 were used in the experiment.

Inducing apoptosis of MSCs and collection technique

When the culture reached 70%-80% confluency, adherent cells were washed 3 times with phosphate-buffered saline without calcium and magnesium (PBS; Takara Bio Inc., Kusatsu, Japan) and then dissociated using TrypLE Express (Gibco, Thermo Fisher Scientific Inc.). As shown in Fig. 1A, a total of 5×10^{5} cells in suspension were then dissolved in a sterile plastic bag filled with 50 ml culture medium, which was subsequently sealed. Those bags were then subjected to pressurization via automated custom made HHP device for 36 h following method described in our previous study (Le at al., unpublished). In brief, when a stable temperature of 36-37 °C was reached in all isostatic chambers, a sealed bag was placed into each chamber, which was then filled with warm tap water and closed tightly. The pressure was then increased to 51 MPa in chambers 1-2-3, while no pressure was applied in chamber 4 (0 MPa, Fig. 1B). After specific pressure magnitude was reach, the countdown was started until 0, at which point the pressure was reduced automatically by the system.

The remain MSCs were parallel cultured in a 10-cm culture dish at 37 °C in a 5% CO_2 incubator for 36 h as a control (Fig. 1E), while MSCs treated with 0.5 μM Staurosporine (STS; #ab120056; Abcam Co., Ltd., MA, USA) for 36 h were used as a reference [27, 28]. After treatment, all of the medium (including cells) in each bag was aspirated and then transferred to 50-ml conical tubes (Falcon, Corning Inc.). After being centrifuged at 1500 g for 3 min, the supernatant was discarded, and the cell pellets were resuspended in 1 ml of fresh medium for downstream investigation. As detection of the appearance of MSC clusters in the 0 MPa_36h group (Fig. 1C), the cell pellets were washed twice with PBS and then detached by 5-min exposure to 0.5 ml of TrypLE Express in the incubator. For STS group, as we found no adherent cells in 10-cm culture dish after 36h treatment (Fig. 1F), the supernatant was aspirated then transferred to 15-ml conical tubes (Falcon, Corning Inc.) and centrifuged for apoMSCs collection.

The flow cytometry analysis of apoMSCs induced by HHP

Briefly, 2-3 × 10^{5} cells per sample were collected and washed 2 times with PBS. For the detection of PtdSer membrane translocation, MSCs were then resuspended in a mixture of 200 μl Assay Buffer, 2 μl

Apopxin Green Indicator, 1 µl 7-AAD and 1 µl CytoCalcein 450 (Apoptosis/Necrosis Detection Kit; #ab176749; Abcam Co., Ltd.) as manual instructions. The samples were then kept protect from light at room temperature (RT) for 30-60 min, and 2×10^4 cells were subsequently archived for flow cytometry analysis on BD FACSCanto II (BD Biosciences, San Jose, CA, USA) using the Flowjo software program (Flowjo LLC, BD Biosciences). The amount of early apoMSCs ($Apopxin^+/7\text{-}AAD^-$) were analyzed and compared.

In addition, after HHP treatment, 1 ml of medium containing approximately 2-3 × 10^5 cells per sample was mixed with 1 µl of CellEvent Caspase-3/7 Green Detection Reagent (CellEvent Caspase-3/7 Green Flow Cytometry Assay Kit; Thermo Fisher Scientific Inc.). The mixture was then vortexed and incubated for 60 min at RT, protected from light. In the final step, 1 µl of 1 mM SYTOX AADvanced dead cell stain solution (CellEvent Caspase-3/7 Green Flow Cytometry Assay Kit; Thermo Fisher Scientific Inc.) was added, and then 2×10^4 cells were archived for analysis on BD FACSCanto II (BD Biosciences) using the Flowjo software program (Flowjo LLC, BD Biosciences).

Immunofluorescence microscopy

Based on our previous method (Le et al., unpublished), 1×10^5 cells per sample were washed with PBS, resuspended in fresh medium, and seeded in a 35-mm glass-bottom dish (Matsunami Glass Ind., Ltd., Osaka, Japan), after which they were stored for 3 hours at 37 °C in a 5% CO_2 incubator to encourage attachment to the dish bottom. For apoptosis/necrosis observation, the medium was gently discarded, and cells were washed 2 times with 200 µl of Assay Buffer. The cells attached to each glass-bottom dish were then incubated with a mixture of 200 µl Assay Buffer, 2 µl Apopxin Green Indicator, 1 µl 7-AAD and 1 µl CytoCalcein 450 (#ab176749; Abcam) at RT for 30-60 min. Finally, images were acquired using a confocal laser scanning microscope by the comibination of Violet, FITC and Alexa Fluor 647 signals (Fluoview FV3000; Olympus Co., Tokyo, Japan).

For measuring DNA fragmentation, we used the DeadEn Fluorometric TUNEL System (#G3250; Promega Corp., WI, USA) following their manual instructions. In brief, 2-3 × 10^5 cells per sample were resuspended in fresh medium, then cultured in a 35-mm glass-bottom dish. After 30-60 min storing in incubator for encougaring dish attachment, those cells were gently washed twice with PBS. Next, they were fixed by 4% methanol-free formaldehyde solution in PBS (pH 7.4) for 25 minutes at 4°C, following immersing in 0.2% Triton X-100 solution for 5 minutes in order to induce cell permeabilization. Next, 200µl of Equilibration Buffer was added to equilibrate at room temperature for 5–10 minutes. After most of Equilibration Buffer was removed by tissue paper, 50 µL of prepared rTdT incubation buffer was added to each sample. The dish was then covered with aluminum foil to protect from light and incubated at 37°C for 60 minutes inside the humidified chamber as allowing the tailing reaction to occur. Stopped reaction by immersing sample in 2X SSC for 15 minutes at RT then washed thrice with PBS for removing unincorporated fluorescein-12-dUTP. Finally, samples were counterstained with Hoestch 33342 solution

(Dojindo Molecular Technologies, Inc., Kumamoto, Japan) and visualized using FV3000 confocal laser microcope.

Identification of pressurized MSCs by TEM

Only the MSCs treated at 0 and 50 MPa for 36 h were observed. The specimens were prepared following the protocol as describe in our previous study [29]. After collection, pressurized or non-pressurized cells were then fixed with fixative solution comprise of 2% glutaraldehyde, 0.1 M sodium cacodylate and 1 mM $CaCl_2$ at 37 °C, pH 7.4 for 30 min. In order to stop fixation, they were then washed 2 times with cacodylate buffer (0.1 M sodium cacodylate and 0.2 M sucrose) at 4 °C, pH 7.4 for 10 min. Next, samples were post-fixed with 1% osmium tetroxide (OsO_4) in cacodylate buffer at 4 °C, pH 7.4 for 30 min and dehydrated by ethanol. After that, they were infiltrated in Epon 812 resin and then polymerized at 45 °C for 12 h, 55 °C for 24 h and 45 °C for 12 h. Consequently, specimens were cut into ultrathin sections and observed by TEM (JEM-1400Plus; JEOL Ltd., Tokyo, Japan).

Viability assessment of MSCs after pressurization

Cell viability can be explored directly through the presence of ubiquitous intracellular esterase activity that cleave moieties from a lipid-soluble nonfluorescent probe to yield a fluorescent product [30]. CytoCalcein 450 is an optimal dye that is sequestered in the cytoplasm of intact membrane cells, thus, is able to distinguish live cells from apoptotic or necrotic cells in whole cell population assessment. By the combination of CytoCalcein Violet 450 staining provided in the Apoptosis/Necrosis Detection Kit (#ab176749; Abcam), we probability detected and analyzed the difference of MSCs viability after treatment. Besides, the LIVE/DEAD Viability/Cytotoxicity Kit (#L-7013, Molecular Probes, Oregon, USA), a basic two-color fluorescence assay for the viability test based on permeability, was additionally used to differentiate live and dead cells. For staining, cell pellets per each sample were immersed in a 200 µL mixture comprise of SYTO 10 Green, DEAD Red in HBSS (1:500 dilution) and incubated in complete darkness for 15 minutes at RT. Next, after centrifugation and supernatant discarding, samples were then fixed with 500 µL of 4% glutaraldehyde in HBSS for 60 minutes. Lastly, samples were centrifuged and removed the fixative; cell pellets were resuspended the in the same volume of HBSS and subjected to analysis on BD FACSCanto II (BD Biosciences) using the Flowjo software program (Flowjo LLC, BD Biosciences).

To assess the irreversible MSCs death and proliferation, adequation 1×10^4 cells in 1 mL culture medium were seeded into a 24-well cell culture plate (Falcon; Corning Inc.) and followed up to 7 days without changing medium in 37 °C/ 5% CO_2 incubator. The morphology and proliferation of culturing MSCs were observed in specific time at 3 h, 1 day, 3 days or 7 days by an inverted microscope (Carl Zeiss Co., Ltd, Oberkochen, Germany). At the same time, WST-8 (Colorimetric Cell Viabilty) assay was used to

quantitatively measured MSCSs proliferation [31, 32]. In brief, a 100-µL aliquot of each cell suspension (1 × 10^4 cells, n=7 per group) was added to four 96-well plate (Falcon; Corning Inc.), then incubated in 37 °C/ 5% CO_2 incubator. At specifc evaluation time point, 10 µL of Cell Counting Kit-8 (CCK-8; Dojindo, Inc.) was added to each well and incubated at 37 °C for 2 h following manufacture instructions. After that, the plate was then gently shaken, and the absorbance of medium was determined at a wavelength of 450 nm using an EnSpire Multimode Plate Reader (PerkinElmer Co., Ltd., Waltham, MA, USA). The absorbance of medium alone in the same well-plate was used as blank (n=7).

Statistical analyses

Results are shown as mean values of at least three independent experiments and standard deviation (SD), represented by bars. Student's *t*-test or Tukey-Kramer post hoc test was used to estimate the significant of differences with Prism software program, ver. 7.03 (GraphPad Software, Inc., San Diego, CA, USA). Values of * p <0.05, ** p <0.01, *** p <0.001, **** p <0.0001 represent the level of significance.

Results

Phosphatidylserine (PtdSer) externalization of pressurized MSCs

As shown in the histogram of Fig. 2A, the Apopxin Green mean fluorescence intensity (MFI) is not only increased in Staurosporine (STS) treatment and 50 MPa_36h, but also increased in 0 MPa_36h group. That could be explained by the sensitive of MSCs in rough condition (closed plastic bag) for long time. However, the Apopxin Green positive proportion is revealed the significant increase in 50 MPa_36h group than 0 MPa_36h group ($p<0.001$), and no specific difference between 50 MPa_36h group and STS group (Fig. 2B). In the Fig. 2C, we can visibly observe the dynamic transition of MSCs from living condition ($FITC^{-ve}$/7-AAD^{-ve}) to apoptotic condition ($FITC^{+ve}$) even in control groups and most of cells are alive MSCs (81.9%). Under inapproriate culturing of 0 MPa_36h, large amount of MSCs became to apoptotic cell death, then we observe the reduction of living MSCs there (42.1%). But, by the impact of hydrostatic pressure (50 MPa_36h group), living MSCs are only around 17.1% and most of cells are apoMSCs, likely in STS group. Consequently, the comparison of early apoptotic cells in Fig. 2D shows the significant higher of early apoMSCs ($FITC^{+ve}$/7-AAD^{-ve}) in 50 MPa_36h group than 0 MPa_36h group ($p<0.05$).

After 3 hours in the live-imaging of apoptosis/necrosis staining (Fig. 2E), we visibly differentiate living MSCs (blue stained), dead MSCs (red stained), late apoMSCs (green and red stained), and early apoMSCs or apoptotic bodies (green stained). The 10x magnification images show the rather similar population of living cells in the control and 0 MPa_36h groups; opposite with most of apoptotic cells (green color) in 50 MPa_36h and STS groups. The higher manification images in control and non-pressurized groups (second row) show more details of living MSCs which identified by spindle shape flattening. A few of apoMSCs or apoptotic bodies can also be observed there. By contrast, in the pressurization or STS groups, we can observe the specific morphology of many apoMSCs with membrane intact, PtdSer

exposure and even the releasing of apoptotic bodies. We also find the positive signals of blue stained cells in both groups and considered those are false positive by evidences proving in viabilty assays. This phenonmenon is related to intracellular esterase activity and was explained in our previous studies [29, 33].

Tranmission Electron Microscopy (TEM) morphology of apoMSCs

Apoptotic cells show a series of physical changes of plasma membrane blebbing, nucleus defragmentation and cell disintegration into apoptotic bodies that are then engulfed and degraded by phagocytes [34, 35]. Since its ultrastructural morphological characteristics is irrefutable, TEM is considered the gold standard for proving apoptosis [36, 37]. As show in Fig. 3, non-pressurized MSCs express distinc of responsibilities after 36h treatment. We found in this group both viable cells (Fig. 3A) and dying cells, including necrotic cell death (Fig. 3B), apoptotic cell death (Fig. 3C) or autophagic cell death (Fig. 3D) [38-40]. Interestingly, in 50 MPa_36h pressurization group, only apoMSCs in different stages of apoptosis were found. Fig. 3E shows the early phase of apoptosis with electron-dense nucleus (pyknosis) and many blebs on cell surface. In the intermediate phase (Fig. 3F), cells nuclear is fragmented (karyorrhexis) and intracellular vacuoles with cytoplasmic organelles inside are formation. Then, in the final stage, apoptotic bodies are released (Fig. 3G), and the hallmark of cell fragmentation was observed (Fig. 3H).

Assessment of caspase activity and nuclear defragmentation in apoMSCs

Caspases play a critical role of protein cleavage in the apoptotic pathway, in which caspase-3 and caspase-7 is considered the most important of the executioner caspases and is activated by any of the initiator caspases. The catalytic activity of executioner caspases is responsible for many of the morphological and biochemical correlates of apoptosis, including DNA fragmentation, PtdSer exposure, and the formation of apoptotic bodies [35, 41]. In the current study, MSCs in closed bags (0 MPa_36h) show higher percentage of activated caspase-3/7 than cells cultured in incubator of control group (28.1% vs 11.4%) (Fig. 4A). However, after treatment at 50 MPa for 36 h, the amount of activated caspase-3/7 in those cells is clearly increasing (69.1%, $p<0.0001$). This result reveal the effective impact of HHP treatment for inducing MSCs apoptosis compare to non-pressurized group or control group.

Another hallmark of apoptosis is internucleosomal cleavage of genomic DNA into small fragments, which were then visualized detection by TdT-mediated dUTP-biotin nick end labeling (TUNEL) assay development. TUNEL staining utilizes the ability of the enzyme terminal deoxynucleotidyl transferase (TdT) to incorporate labeled dUTP onto the free 3’-hydroxyl termini of fragmented genomic DNA [42, 43]. As shown in Fig. 4B, the fluorometric TUNEL stained indicate that plenty of MSCs in 50 MPa_36h or STS treatment groups have DNA fragmentations, while a few ones were found in control and

0 MPa_36h groups. Furthermore, oval shaped, intact membrane nuclei which stained by Hoestch 33342 show that most of cells in control and 0 MPa_36h group are alive cells. By contrast, nuclear morphology changes of MSCs in 50 MPa_36h and STS group suggest that most of them are dying cells.

Viability assessments of pressurized MSCs

We used CytoCalcein 450 staining in Apoptosis/Necrosis assay (#ab176749, Abcam) and Live/Dead staining (L-7013, Molecular Probes) for investigation of MSCs viability after pressurization. As shown in Fig. 5A, the CytoCalcein 450 histogram show not seriously difference of cells survival between MSCs in 0 MPa_36h and control groups, but totally different from its survial in 50 MPa_36h or STS treatment. Consequently, the ratio of CytoCalcein 450 positive of MSCs in 50 MPa_36h or STS treatment are actually lower than MSCs in 0 MP_36h (13.3% vs 61.7%, $p<0.0001$, n=3) and in control group (13.3% vs 93.4%, $p<0.0001$, n=3). Additionally, in Live/Dead staining assay, SYTO 10, a green fluorescent nucleic acid stain, is a highly membrane-permeant dye and labels all cells, including those with intact plasma membranes. As shown in Fig. 5B of SYTO 10 expression, we observe the similarity of MSCs nuclei stained in control and 0 MPa_36h groups, but profoundly different in 50 MPa_36h group. That could be explained due to nuclear fragmentation happen in apoMSCs of pressurized group. In contrast, DEAD Red is a cell-impermeant fluorescent nucleic acid stain that labels only cells with compromised membranes (refer as dead cells). The results of that staining in Fig. 5B indicate that around 33% of MSCs in 0 MPa_36h group are dead compare with around 78% of death MSCs found in 50 MPa_36h group ($p<0.0001$, n=3).

In addition, WST-8 assay and inverted microscopy observation were used to confirm the completely irreversible MSCs death and proliferation. As shown in Fig. 5C, we found that the MSCs in the 0 MPa_36h group were markedly weaker than those in the control group at 3 h after culturing, but subsequently proliferated alongside with normal MSCs in control group until day 7. Nonetheless, neither signal of viable MSCs in 50 MPa_36h or STS treatment group was detected up to 7 days of cells seeding. Besides, live-imaging microscopic observation of pressurized MSCs (Fig. 5D) reveal that no alive cell was detected in 50 MPa_36h and STS groups for all period of time assessment, while most of MCSs in 0 MPa_36h group were viable, remain original characteristics and well proliferated likely normal MSCs (control group) over the time. As a consequence, we considered that persistent HHP treatment at 50 MPa truly induce MSCs death.

Discussion

Numerous studies have reported that apoptosis usually happens after HHP treatment around 100 MPa. This phenonmenon was observed on many cell lines, including murine erythroleukemia (MEL) cells, human lymphoblasts, B35, PC12 and retinal gangalion cell lines [25]. The molecular biology of high pressure-induced apoptosis was demonstrated through the activation of caspase-3, via both extrinsic and intrinsic pathways [44]. In the current study, we confirmed the appearance of cleavaged caspase-3/7, executioner caspases are considered irreversible and playing critical role for all morphological changes of

apoptotic cells, including DNA fragmentation and PtdSer membrane exposure [41, 45]. As shown in Fig. 4A, besides the clear elevation of activated caspase-3/7 of apoMSCs in 50 MPa_36h, that elevation is also observed in 0 MPa_36h group. It indicated that suspended culture condition in closed bag for long time contributed to stimulate programmed cell death of MSCs there. The causes might be the comorbidity of any non-optimal culture conditions, including nutrient starvation, pH changes, hypoxia, cell aggregation and vice versa [46]. Accordingly, MSCs in 0 MPa_36h group can be spontanously triggered to necrosis, apoptosis, or autophagy which their ultrastructure morphology are observed in figure 3B-3D. Is that condition impact to effect of our persistent HHP treatment? Notably, we did not find any above phenomenons of MSCs death in 50 MPa_36h group, excepted apoptotic bodies and different morphological stages of apopMSCs (Fig. 3E-3H). That is unclear to explain the impact of hydrostatic pressure only or concomitant impact of all factors inside cause the affect and need to investigate in further study.

As shown in Fig. 4B, the TUNEL staining result clearly demonstrates the diffecence of MSCs with/without pressurization after 36 hours treatment. Indeed, we detected diversity of TUNEL signals (FITC positive) of apoMSCs in 50 MPa group similar to those in STS treatment. Although TUNEL staining is very sensitive by the ability of single cell detection via fluorescence microscopy, it is important to recognize that this staining is not limited to the detection of apoptotic cells [47]. Because TUNEL stained is non-specific label all free 3'-hydroxyl termini, it will also detect non-apoptotic cells including necrotic degenerating cells, cells undergoing DNA repair, cells damaged by mechanical forces, and even cells undergoing active gene transcription. Therefore, it should be considered generally as a method for the detection of DNA damage (DNA fragmentation or others), and more specifically when used in conjunction with secondary apoptosis-specific assays [42].

Apoptosis has been considered a form of 'silent' cell death for a long time, in contrast to necrosis, which frequently induces inflammation by releasing danger-associated molecular patterns (DAMPs). However, this notion has changed, and apoptosis has gradually been shown to participate in communication with neighboring cells to contribute to survival or apoptosis and remodeling of the surrounding tissues [11]. Our previous study reported that apoptotic cells in inactivated murine skin attracted macrophages ($F4/80^+$) migration in *in vivo* transplantaion and subsequently promoted its wound healing regeneration (Le et al., unpublished). As apoptotic cells, we considered pressurized MSCs after infusion will attract phagocytes by 'find me' signals, then phagocytic uptake (refer as efferocytosis) by phosphatidylserine membrane exposure [48]. In the paper "dying stem cell hypothesis", Thum et al. proposed that the efferocytosis of apoMSCs may causes a down-regulation of the innate and adaptive immunity in local immune response [8]. In consistent with that hypothesis, it was reported that apoptotic adipose-derived MSCs treatment is superior to living MSCs in a cecal ligation and puncture (CLP)-induced sepsis model in rats. The parameters for sepsis-induced acute lung injury (ALI) and acute kidney injury were significantly lower in the group treated with apoptotic MSCs [9, 10]. Additionally, extracellular vesicles (Evs) derived from MSCs (MSC-EVs) is believed to regulate apoptosis, cell proliferation, and express many angiogenesis-promoting molecules, including IL-6, basic fibroblast growth factor (bFGF), vascular

endothelial growth factor (VEGF), monocyte chemoattractant protein (MCP-1) and the VEGF receptor-2 [49]. In comparison to whole cell-based therapies, MSC-EVs were reported more specific advantages for patient safety such as lower propensity to trigger innate and adaptive immune responses or inability to directly form tumors. Recent animal model-based studies suggest that EVs have significant potential as a novel alternative therapies in various disease, including cardiovascular, acute kidney injury (AKI), endotoxin-induced acute lung injury (ALI), liver disease and so on [50]. Accordingly, diversity of biotechnology and cell therapy industries are currently attempting to develop this subcellular therapeutic machinery (in a naïve or modified state) for regenerative medicine, as substitutes for intact cell therapy, and as intelligent targeted drug delivery carriers [13].

Conclusions

In this study, our data shows that HHP treatment is convenient processing which effectively induce MSCs undergo to apoptosis. Further, this processing is considered safety as using not any chemical reagents, leading to simply manufacturing prapared products for industrial therapies. We hope that our findings might contribute to improve mesenchymal stem/stromal cells as well as extracellular vesicles in translational research development.

Abbreviations

Apoptotic MSCs: apoMSCs; CAFs: carcinoma associated fibroblasts; DAMPs: danger-associated molecular patterns; EVs: extracellular vesicles; HHP: high hydrostatic pressure; MSCs: mesenchymal stem cells; MSC-EVs: MSC-derived extracellular vesicles; PtdSer: phosphotidylserine; STS: Staurosporine; TEM: Transmission electron microscopy; TUNEL: terminal deoxynucleotidyl transferase dUTP nick-end labeling.

Declarations

Ethics approval

Not applicable.

Consent for publication

All authors provide consent for publication of this manuscript.

Availability of data and materials

All data generated or analysed during this study are included in this published article.

Authors' contribution

T.M.L performed and designed experiments, analyzed data, wrote paper; N.M. conceived the study, interpreted data, and wrote the paper; N.T.M.L helped to perform experiments and analyzed data. T.M conducted pressurization and Tranmission Electron Microscopy experiments. S.C.N analyzed data and help to draft paper. N.K. helped to interpret data and edit the paper; K.K. contributed to the conceptual design and helped to wrote paper. All authors approved for paper submission. N.M. is the grant recipient.

Fundings

This research was partially supported by Grants-in-Aid for Scientific Research (B) (17H04360) (https://kaken.nii.ac.jp/ja/index/) and by a Practical Research for Innovative Cancer Control grant (17ck0106304h0001) Agency for Medical Research and Development (AMED; http://www.amed.go.jp/en/); Dr. Naoki Morimoto. The funders had no role in study design, data collection and analysis, decision to publish, or preparation of the manuscript.

Acknowledgements

We are grateful to Japan Tissue Engineering Co., Ltd. (J-TEC) for kindly supplying bone-marrow MSCs and BMP01(-) cell culture medium. We are also grateful to Akira Saito for his technical assistance in Tranmission Electron Microscopy (TEM) experiment.

Competing Interests: The authors declare that they have no competing interests.

References

[1] A.I. Caplan, Mesenchymal stem cells, Journal of orthopaedic research : official publication of the Orthopaedic Research Society, 9 (1991) 641-650.

[2] P. Bianco, P.G. Robey, P.J. Simmons, Mesenchymal stem cells: revisiting history, concepts, and assays, Cell Stem Cell, 2 (2008) 313-319.

[3] J. Galipeau, L. Sensebe, Mesenchymal Stromal Cells: Clinical Challenges and Therapeutic Opportunities, Cell Stem Cell, 22 (2018) 824-833.

[4] K. Le Blanc, O. Ringden, Immunomodulation by mesenchymal stem cells and clinical experience, J Intern Med, 262 (2007) 509-525.

[5] E. Eggenhofer, V. Benseler, A. Kroemer, F.C. Popp, E.K. Geissler, H.J. Schlitt, C.C. Baan, M.H. Dahlke, M.J. Hoogduijn, Mesenchymal stem cells are short-lived and do not migrate beyond the lungs after intravenous infusion, Front Immunol, 3 (2012) 297.

[6] S.F.H. de Witte, F. Luk, J.M. Sierra Parraga, M. Gargesha, A. Merino, S.S. Korevaar, A.S. Shankar, L. O'Flynn, S.J. Elliman, D. Roy, M.G.H. Betjes, P.N. Newsome, C.C. Baan, M.J. Hoogduijn, Immunomodulation By Therapeutic Mesenchymal Stromal Cells (MSC) Is Triggered Through Phagocytosis of MSC By Monocytic Cells, Stem Cells, 36 (2018) 602-615.

[7] A. Galleu, Y. Riffo-Vasquez, C. Trento, C. Lomas, L. Dolcetti, T.S. Cheung, M. von Bonin, L. Barbieri, K. Halai, S. Ward, L. Weng, R. Chakraverty, G. Lombardi, F.M. Watt, K. Orchard, D.I. Marks, J. Apperley, M. Bornhauser, H. Walczak, C. Bennett, F. Dazzi, Apoptosis in mesenchymal stromal cells induces in vivo recipient-mediated immunomodulation, Science translational medicine, 9 (2017).

[8] T. Thum, J. Bauersachs, P.A. Poole-Wilson, H.D. Volk, S.D. Anker, The dying stem cell hypothesis: immune modulation as a novel mechanism for progenitor cell therapy in cardiac muscle, J Am Coll Cardiol, 46 (2005) 1799-1802.

[9] P.-H. Sung, C.-L. Chang, T.-H. Tsai, L.-T. Chang, S. Leu, Y.-L. Chen, C.-C. Yang, S. Chua, K.-H. Yeh, H.-T. Chai, H.-W. Chang, H.-H. Chen, H.-K. Yip, Apoptotic adipose-derived mesenchymal stem cell therapy protects against lung and kidney injury in sepsis syndrome caused by cecal ligation puncture in rats, Stem Cell Research & Therapy, 4 (2013) 155.

[10] A.R.R. Weiss, M.H. Dahlke, Immunomodulation by Mesenchymal Stem Cells (MSCs): Mechanisms of Action of Living, Apoptotic, and Dead MSCs, Front Immunol, 10 (2019) 1191.

[11] R. Kakarla, J. Hur, Y.J. Kim, J. Kim, Y.J. Chwae, Apoptotic cell-derived exosomes: messages from dying cells, Exp Mol Med, 52 (2020) 1-6.

[12] S. Caruso, I.K.H. Poon, Apoptotic Cell-Derived Extracellular Vesicles: More Than Just Debris, Front Immunol, 9 (2018) 1486.

[13] V. Agrahari, V. Agrahari, P.A. Burnouf, C.H. Chew, T. Burnouf, Extracellular Microvesicles as New Industrial Therapeutic Frontiers, Trends Biotechnol, 37 (2019) 707-729.

[14] W. Zhu, W. Xu, R. Jiang, H. Qian, M. Chen, J. Hu, W. Cao, C. Han, Y. Chen, Mesenchymal stem cells derived from bone marrow favor tumor cell growth in vivo, Exp Mol Pathol, 80 (2006) 267-274.

[15] F. Djouad, P. Plence, C. Bony, P. Tropel, F. Apparailly, J. Sany, D. Noel, C. Jorgensen, Immunosuppressive effect of mesenchymal stem cells favors tumor growth in allogeneic animals, Blood, 102 (2003) 3837-3844.

[16] Y. Shi, L. Du, L. Lin, Y. Wang, Tumour-associated mesenchymal stem/stromal cells: emerging therapeutic targets, Nat Rev Drug Discov, 16 (2017) 35-52.

[17] E.L. Spaeth, J.L. Dembinski, A.K. Sasser, K. Watson, A. Klopp, B. Hall, M. Andreeff, F. Marini, Mesenchymal stem cell transition to tumor-associated fibroblasts contributes to fibrovascular network expansion and tumor progression, PloS one, 4 (2009) e4992.

[18] P.J. Mishra, P.J. Mishra, R. Humeniuk, D.J. Medina, G. Alexe, J.P. Mesirov, S. Ganesan, J.W. Glod, D. Banerjee, Carcinoma-Associated Fibroblast-Like Differentiation of Human Mesenchymal Stem Cells, Cancer Research, 68 (2008) 4331-4339.

[19] A. Adamo, G. Dal Collo, R. Bazzoni, M. Krampera, Role of mesenchymal stromal cell-derived extracellular vesicles in tumour microenvironment, Biochim Biophys Acta Rev Cancer, 1871 (2019) 192-198.

[20] S. Bruno, F. Collino, A. Iavello, G. Camussi, Effects of mesenchymal stromal cell-derived extracellular vesicles on tumor growth, Front Immunol, 5 (2014) 382.

[21] T.S. Cheung, A. Galleu, M. von Bonin, M. Bornhäuser, F. Dazzi, Apoptotic mesenchymal stromal cells induce prostaglandin E2 in monocytes: implications for the monitoring of mesenchymal stromal cell activity, Haematologica, 104 (2019) e438-e441.

[22] V.V. Mozhaev, K. Heremans, J. Frank, P. Masson, C. Balny, Exploiting the effects of high hydrostatic pressure in biotechnological applications, Trends in Biotechnology, 12 (1994) 493-501.

[23] B. Frey, S. Franz, A. Sheriff, A. Korn, G. Bluemelhuber, U.S. Gaipl, R.E. Voll, R. Meyer-Pittroff, M. Herrmann, Hydrostatic pressure induced death of mammalian cells engages pathways related to apoptosis or necrosis, Cellular and molecular biology (Noisy-le-Grand, France), 50 (2004) 459-467.

[24] A. Aertsen, F. Meersman, M.E. Hendrickx, R.F. Vogel, C.W. Michiels, Biotechnology under high pressure: applications and implications, Trends Biotechnol, 27 (2009) 434-441.

[25] N. Rivalain, J. Roquain, G. Demazeau, Development of high hydrostatic pressure in biosciences: pressure effect on biological structures and potential applications in biotechnologies, Biotechnol Adv, 28 (2010) 659-672.

[26] A. Isidan, S. Liu, P. Li, M. Lashmet, L.J. Smith, H. Hara, D.K.C. Cooper, B. Ekser, Decellularization methods for developing porcine corneal xenografts and future perspectives, Xenotransplantation, 26 (2019) e12564.

[27] C.A. Belmokhtar, J. Hillion, E. Ségal-Bendirdjian, Staurosporine induces apoptosis through both caspase-dependent and caspase-independent mechanisms, Oncogene, 20 (2001) 3354.

[28] J. Leibacher, K. Dauber, S. Ehser, V. Brixner, K. Kollar, A. Vogel, G. Spohn, R. Schafer, E. Seifried, R. Henschler, Human mesenchymal stromal cells undergo apoptosis and fragmentation after intravenous application in immune-competent mice, Cytotherapy, 19 (2017) 61-74.

[29] T. Mitsui, N. Morimoto, A. Mahara, S.C. Notodihardjo, T.M. Le, M.C. Munisso, M. Moriyama, H. Moriyama, N. Kakudo, T. Yamaoka, K. Kusumoto, Exploration of the Pressurization Condition for Killing Human Skin Cells and Skin Tumor Cells by High Hydrostatic Pressure, BioMed Research International, 2020 (2020) 1-17.

[30] S. Johnson, V. Nguyen, D. Coder, Assessment of cell viability, Curr Protoc Cytom, Chapter 9 (2013) Unit9 2.

[31] T.L. Riss, R.A. Moravec, A.L. Niles, S. Duellman, H.A. Benink, T.J. Worzella, L. Minor, Cell Viability Assays, in: G.S. Sittampalam, N.P. Coussens, K. Brimacombe, A. Grossman, M. Arkin, D. Auld, C. Austin, J. Baell, B. Bejcek, J.M.M. Caaveiro, T.D.Y. Chung, J.L. Dahlin, V. Devanaryan, T.L. Foley, M. Glicksman, M.D. Hall, J.V. Haas, J. Inglese, P.W. Iversen, S.D. Kahl, S.C. Kales, M. Lal-Nag, Z. Li, J. McGee, O. McManus, T. Riss, O.J. Trask, Jr., J.R. Weidner, M.J. Wildey, M. Xia, X. Xu (Eds.) Assay Guidance Manual, Bethesda (MD), 2016.

[32] K. Chamchoy, D. Pakotiprapha, P. Pumirat, U. Leartsakulpanich, U. Boonyuen, Application of WST-8 based colorimetric NAD(P)H detection for quantitative dehydrogenase assays, BMC Biochemistry, 20 (2019).

[33] A. Mahara, N. Morimoto, T. Sakuma, T. Fujisato, T. Yamaoka, Complete cell killing by applying high hydrostatic pressure for acellular vascular graft preparation, Biomed Res Int, 2014 (2014) 379607.

[34] A. Tinari, A.M. Giammarioli, V. Manganelli, L. Ciarlo, W. Malorni, Analyzing morphological and ultrastructural features in cell death, Methods Enzymol, 442 (2008) 1-26.

[35] L. Galluzzi, I. Vitale, Molecular mechanisms of cell death: recommendations of the Nomenclature Committee on Cell Death 2018, Cell death and differentiation, 25 (2018) 486-541.

[36] S. Elmore, Apoptosis: A Review of Programmed Cell Death, Toxicologic pathology, 35 (2007) 495-516.

[37] M.K. White, C. Cinti, A morphologic approach to detect apoptosis based on electron microscopy, Methods in molecular biology (Clifton, N.J.), 285 (2004) 105-111.

[38] V. Nikoletopoulou, M. Markaki, K. Palikaras, N. Tavernarakis, Crosstalk between apoptosis, necrosis and autophagy, Biochim Biophys Acta, 1833 (2013) 3448-3459.

[39] Y. Tsujimoto, S. Shimizu, Another way to die: autophagic programmed cell death, Cell death and differentiation, 12 Suppl 2 (2005) 1528-1534.

[40] U. Ziegler, P. Groscurth, Morphological features of cell death, News Physiol Sci, 19 (2004) 124-128.

[41] K. Segawa, S. Kurata, Y. Yanagihashi, T.R. Brummelkamp, F. Matsuda, S. Nagata, Caspase-mediated cleavage of phospholipid flippase for apoptotic phosphatidylserine exposure, Science, 344 (2014) 1164-1168.

[42] D.T. Loo, In situ detection of apoptosis by the TUNEL assay: an overview of techniques, Methods in molecular biology (Clifton, N.J.), 682 (2011) 3-13.

[43] C.D. Bortner, N.B.E. Oldenburg, J.A. Cidlowski, The role of DNA fragmentation in apoptosis, Trends in Cell Biology, 5 (1995) 21-26.

[44] T. Yamaguchi, K. Hashiguchi, S. Katsuki, W. Iwamoto, S. Tsuruhara, S. Terada, Activation of the intrinsic and extrinsic pathways in high pressure-induced apoptosis of murine erythroleukemia cells, Cell Mol Biol Lett, 13 (2008) 49-57.

[45] S. Nagata, J. Suzuki, K. Segawa, T. Fujii, Exposure of phosphatidylserine on the cell surface, Cell death and differentiation, 23 (2016) 952-961.

[46] L. Galluzzi, M.C. Maiuri, I. Vitale, H. Zischka, M. Castedo, L. Zitvogel, G. Kroemer, Cell death modalities: classification and pathophysiological implications, Cell death and differentiation, 14 (2007) 1237-1243.

[47] M. Watanabe, M. Hitomi, K. van der Wee, F. Rothenberg, S.A. Fisher, R. Zucker, K.K. Svoboda, E.C. Goldsmith, K.M. Heiskanen, A.L. Nieminen, The pros and cons of apoptosis assays for use in the study of cells, tissues, and organs, Microsc Microanal, 8 (2002) 375-391.

[48] M.R. Elliott, K.S. Ravichandran, The Dynamics of Apoptotic Cell Clearance, Dev Cell, 38 (2016) 147-160.

[49] J. Chen, Z. Liu, M.M. Hong, H. Zhang, C. Chen, M. Xiao, J. Wang, F. Yao, M. Ba, J. Liu, Z.K. Guo, J. Zhong, Proangiogenic compositions of microvesicles derived from human umbilical cord mesenchymal stem cells, PloS one, 9 (2014) e115316.

[50] S. Rani, A.E. Ryan, M.D. Griffin, T. Ritter, Mesenchymal Stem Cell-derived Extracellular Vesicles: Toward Cell-free Therapeutic Applications, Mol Ther, 23 (2015) 812-823.

Figures

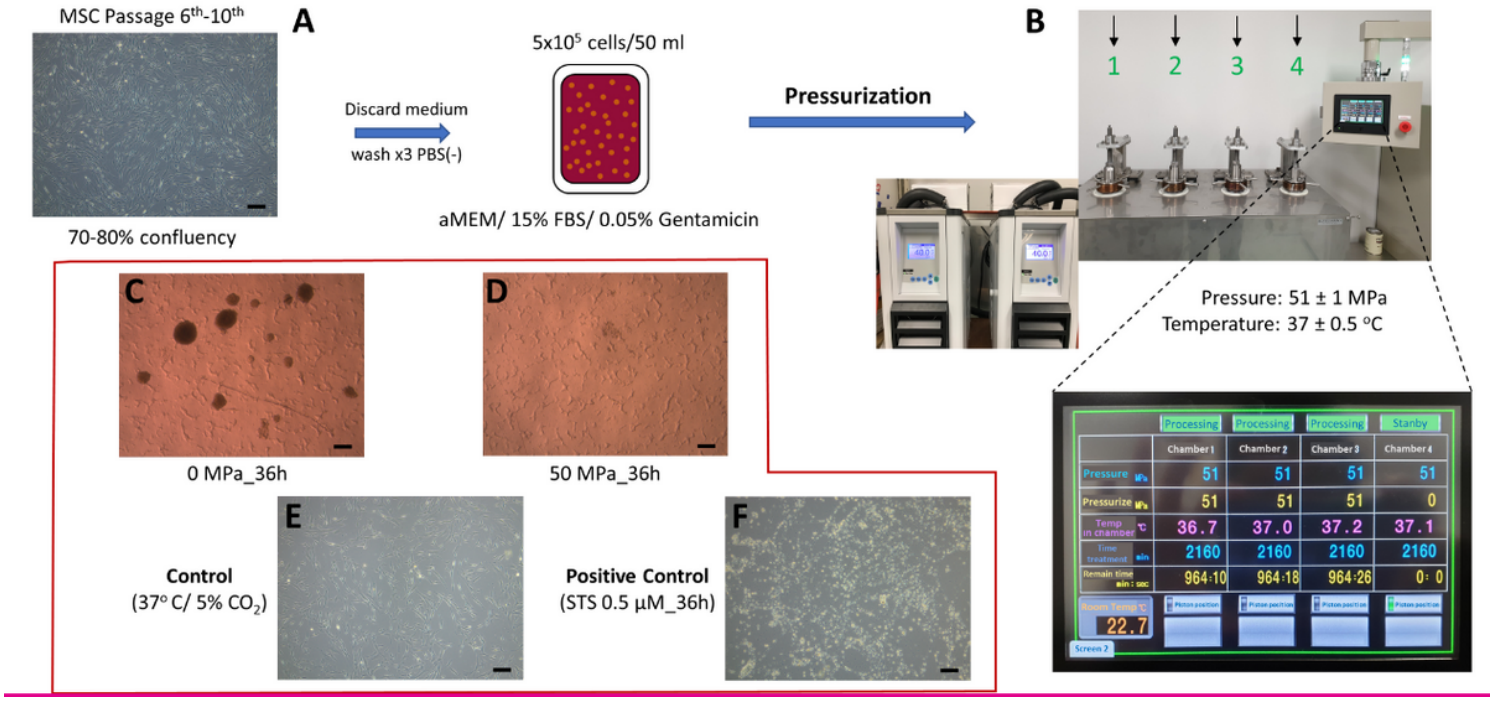

Figure 1

Schematic description of the pressurization processing. Adherent MSCs after several passages (A) in incubator were trypsinazed and transited to suspend culture in a sealed plastic bag. Each bag was transfered to isostatic chamber (No. 1-4) filled with warmed up tap water then pressurized via automated HHP device (B). The enlarge screen monitor shows the input setting and status of environments condition inside each chamber. Timer countdowns start after setting pressure magnitude reached and the system automatically reduces pressure to 0 when finish. Immediately after pressurization, a lot of viable MSC clusters were found in 0 MPa_36h group (C), but only cell debris was shown in 50 MP_36h group (D). Microscopic images show the difference between MSCs in incubator (control, E) and MSCs treated with STS (positive control, F).

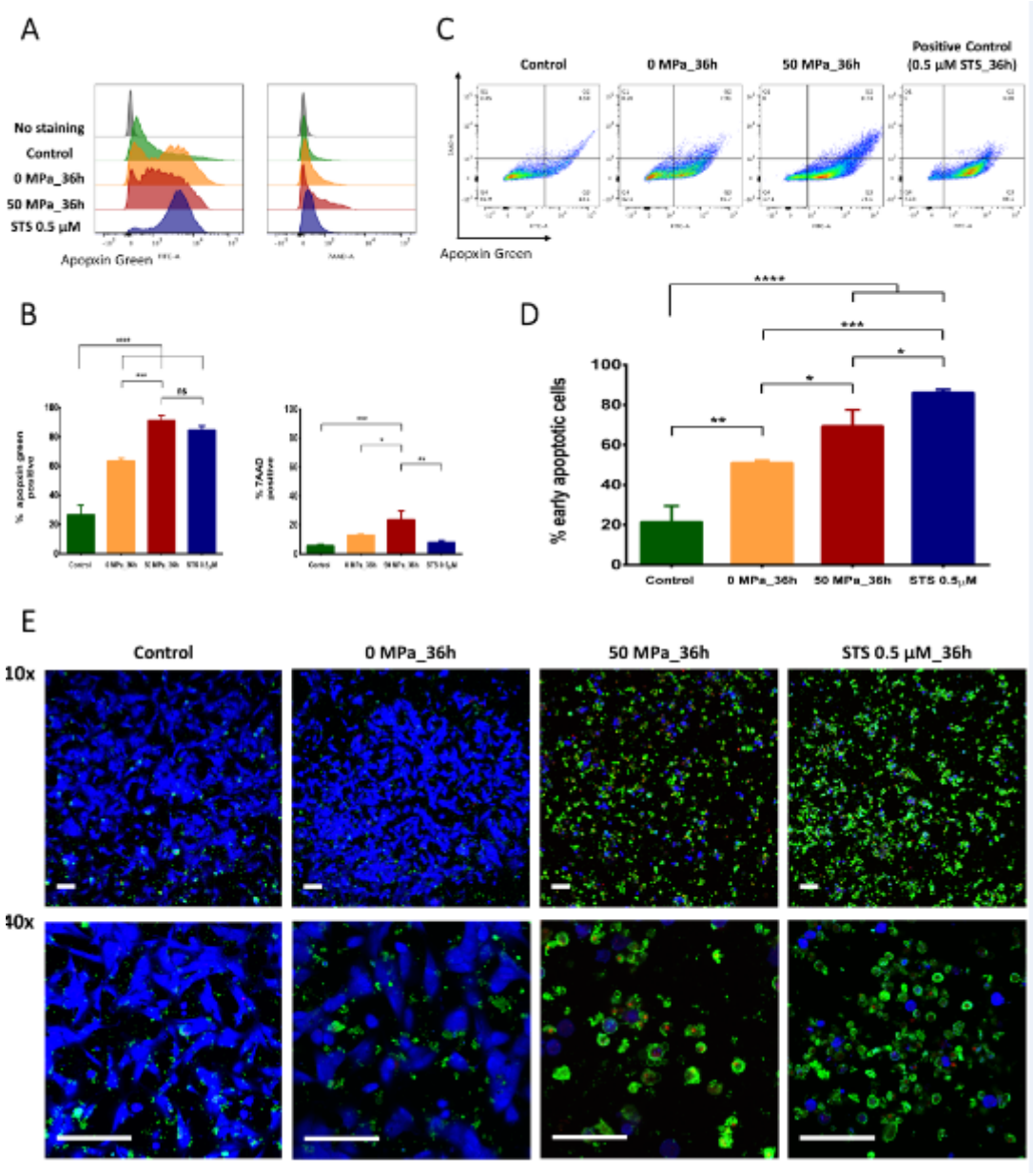

Figure 2

Detection of phosphatidylserine (PtdSer) externalization of pressurized MSCs. (A) Representative histograms of Apopxin Green (FITC) shows the different fluorescence expression of 0 MPa, 50 MPa and STS groups compare with control group. However, different fluorescence of 7-AAD is not clear. Data are representative of three independent experiments. (B) The comparison of Apopxin Green positive propotion reveals the significantly increasing in all treatment groups than control ($p<0.0001$, $n=3$). The positive ratio of FITC in pressurized group is higher than non-pressurized group and not specfic different with STS treament group. The 7-AAD positive proportion of 50 MPa_36h group is higher than other groups too ($p<0.05$, $n=3$). (C) The flow cytometer diagram formed by the combination of Apopxin Green-FITC and 7-AAD immunofluorescence visibly show the dynamic transition of MSCs from living (FITC-ve/7-AAD-ve) to apoptotic condition (FITC+ve) even in control groups. In 0 MPa_36h group, half of MSCs undergo apoptosis, while around 80% of apoMSCs are found in 50 MPa_36h group. Notably, most of

cells in STS group are apoMSCs. Data are representative of three independent experiments. (D) The comparison of early apoMSCs (FITC+ve/7-AAD-ve) shows the clearly different between control group and 50 MPa_36h or STS treatment group ($p<0.0001$, n=3). The amount of apoMSCs in 0 MPa_36h higher than control group ($p<0.01$, n=3), but lower than 50 MPa_36h group ($p<0.05$, n=3). (E) Immunofluorescence microscopic images of apoptosis/necrosis staining show the different intensity of living MSCs (blue color) and apoMSCs (green/red color) or dead MSCs (red color) in 10x magnification among groups. Higher 40x magnifications images show more morphological characteristics of living MSCs which identified by spindle shape flattening, while a few of apoMSCs or apoptotic bodies observed in control and 0 MPa_36h group. By contrast, many apoMSCs with membrane intact, PtdSer exposure and even the releasing of apoptotic bodies were found in the 50 MPa_36h or STS groups. Data are representative of at least three independent experiments.

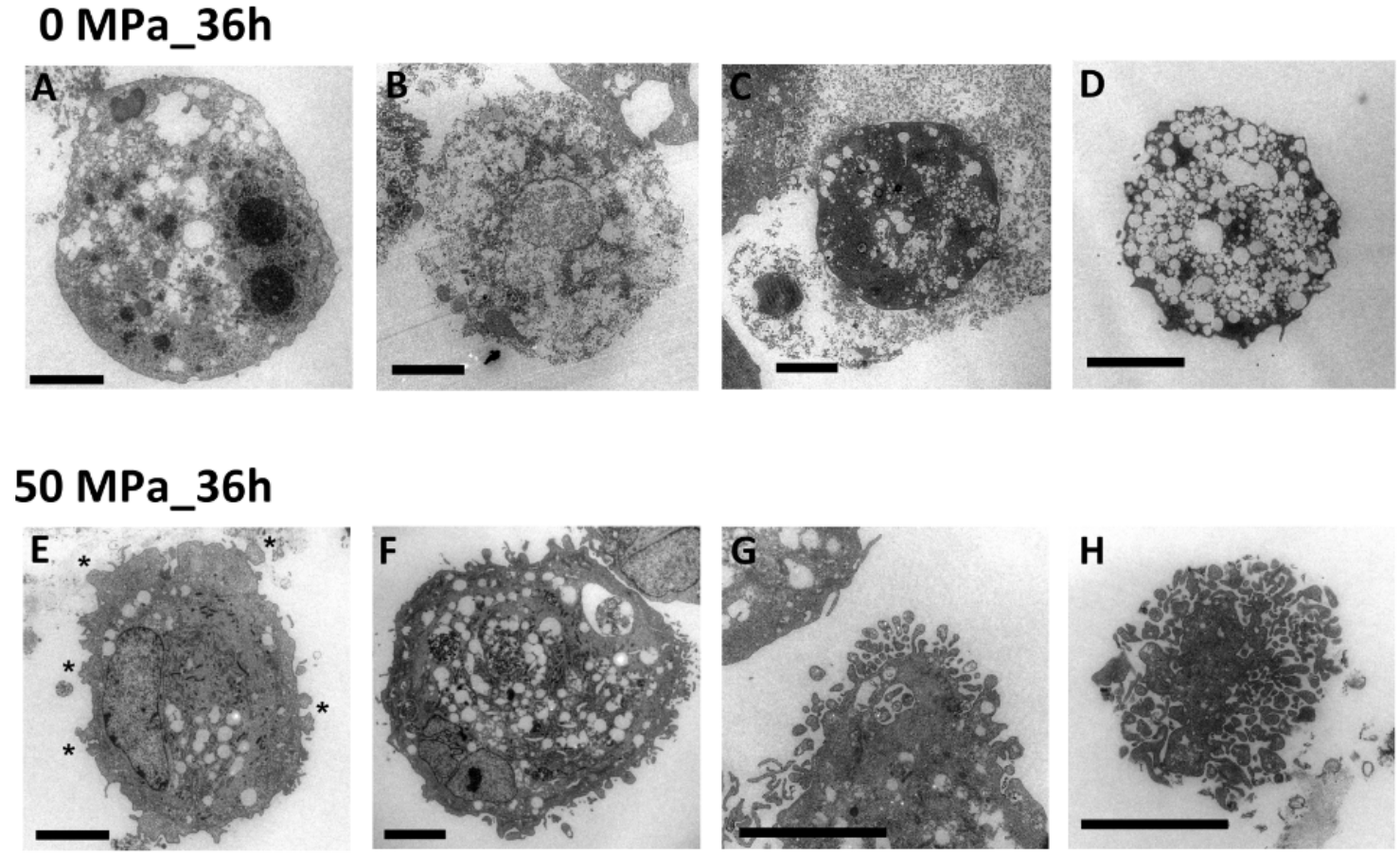

Figure 3

Tranmission Electron Microscopy (TEM) morphology of MSCs. In non-pressurization group: (A) living MSC exhibited a normal morphology with intact membrane, scant cytoplasm, and round nuclei; (B) necrotic MSC with nucleus disintegrates, organelles dilation, membrane permeabilization and rupture; (C) apoptotic MSC with intact membrane, nuclear fragments, formed of intracellular vacuoles and apoptotic bodies; (D) autophagic MSC exhibited intact membrane, the absence of chromatin condensation, autophagosomes and autolysosomes formation in the cytoplasm. In 50 MPa_36h pressurization group, only apoMSCs in different stages of apoptosis were found: (E) the early phase of apoptosis with reducing

of cytoplasmic organelles, electron-dense nucleus (pyknosis) and plasma membrane blebbing (asterisks); (F) the intermediate phase reveals fragmented nuclear (karyorrhexis) and the formation of intracellular vacuoles with cytoplasmic organelles inside. (G) the final stage shows apoptotic bodies are releasing; and (H) the hallmark of whole cell fragmentation in the last. Magnification 6000X – 12000X, scale bar: 5 µm.

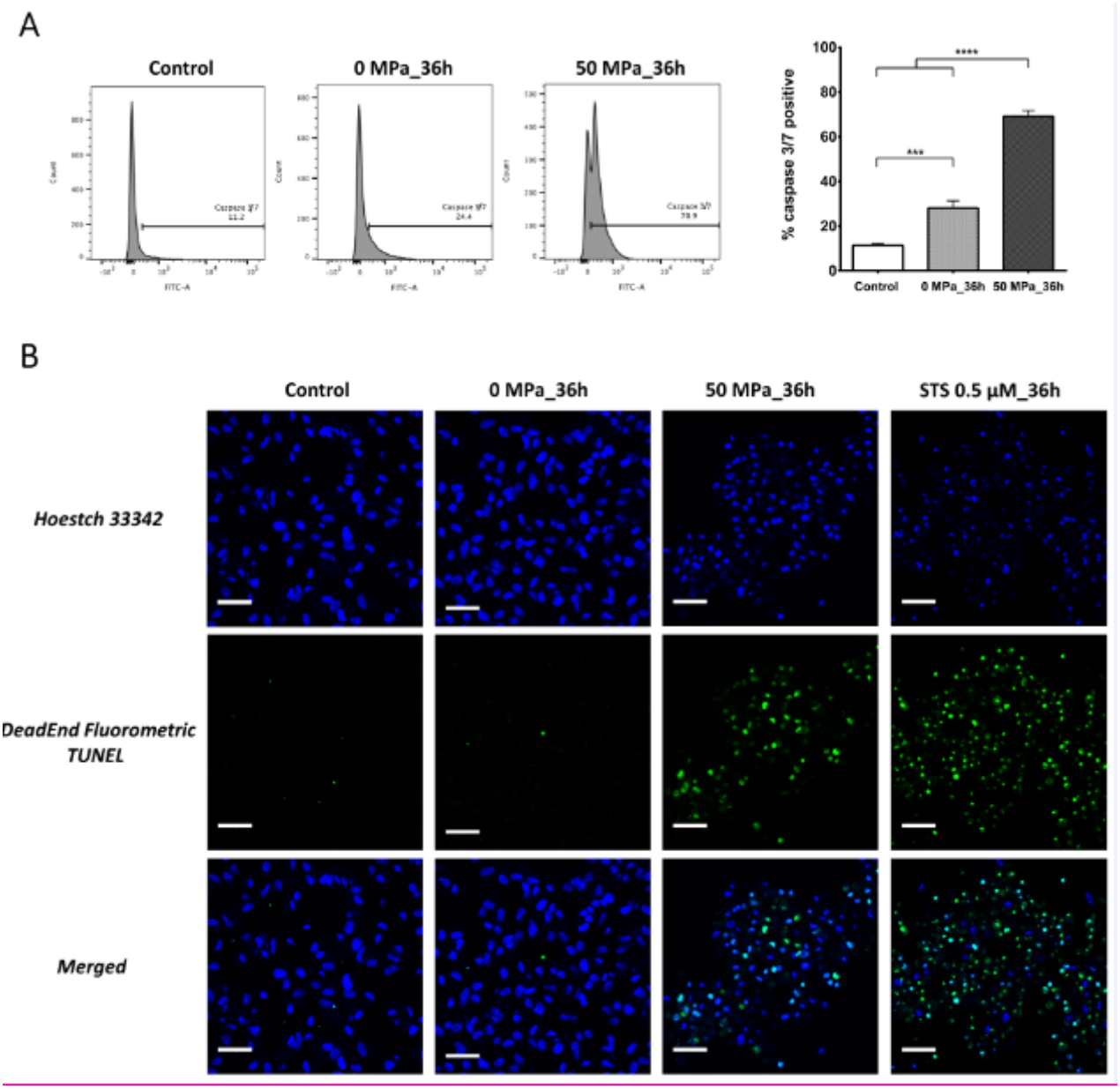

Figure 4

Nuclear defragmentation and activated caspase-3/7 involve in HHP treatment (A) Representative flow cytometry histogram shows higher percentage of activated caspase-3/7 positive expressed in MSCs of 0 MPa_36h group than control group (28.1% vs 11.4%, p< 0.001, n=3). By effect of pressurization at 50 MPa for 36 h, the amount of activated caspase-3/7 detected in MSCs is clearly increasing than non-pressure group (69.1%, p<0.0001, n=3). (B) The DeadEnd Fluorometric TUNEL stained shows that plenty of MSCs in 50 MPa_36h or STS treatment groups have DNA fragmentations, while a few ones were found in control and 0 MPa_36h groups. Addtionally, oval shaped, intact nuclei which counterstained by

Hoestch 33342 reveal that most of MSCs in control and 0 MPa_36h group are alive cells. By contrast, nuclear morphology changes of MSCs in 50 MPa_36h and STS group suggest that they are dying cells. Data are representative of three independent experiments.

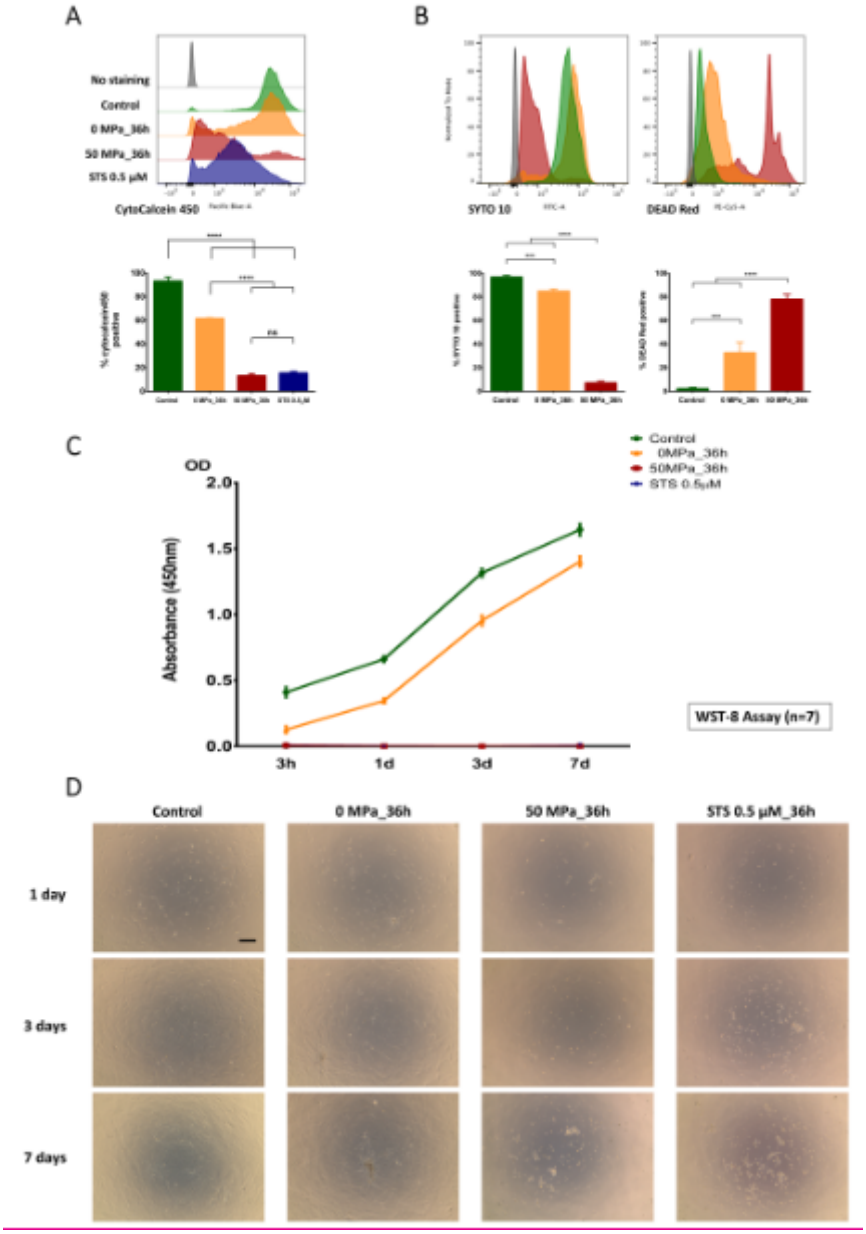

Figure 5

Viability assessment of MSCs after pressurization. (A) The representative CytoCalcein 450 histogram show not seriously difference of cells survival between MSCs in 0 MPa_36h and control groups, which totally different from its survial in 50 MPa_36h or STS treatment. As a results, the ratio of CytoCalcein 450 positive of MSCs in 50 MPa_36h or STS treatment are actually lower than MSCs in 0 MP_36h (13.3% vs 61.7%, $p<0.0001$, n=3) and in control group (13.3% vs 93.4%, $p<0.0001$, n=3). (B) The SYTO 10 fluorescence histogram and positive ratio comparison reveal the similarity of MSCs nuclei stained in control and 0 MPa_36h groups, but profoundly different in 50 MPa_36h group ($p<0.0001$, n=3). In contrast, is a cell-impermeant fluorescent nucleic acid stain that labels only cells with compromised

membranes (refer as dead cells). The results of DEAD Red staining indicate that around 33% of MSCs in 0 MPa_36h group are dead cells compare with around 78% of death MSCs found in 50 MPa_36h group ($p<0.0001$, $n=3$). (C) Absorbance measuring at 450 nm in the WST-8 assay shows that MSCs in 0 MPa_36h group were markedly weaker than those in the control group at 3 h after culturing, but subsequently proliferated alongside with normal MSCs in control group until day 7. Nonetheless, neither signal of viable MSCs in 50 MPa_36h or STS treatment group was detected up to 7 days of cells seeding. Data are representative of two independent experiments. (D) Live-imaging microscopic observation reveal that no alive cell was detected in 50 MPa_36h and STS groups for all period of time assessment, while a lot of MCSs in 0 MPa_36h group were viable, remain original characteristics and well proliferated likely normal MSCs (control group) over the time. Magnification 4x, scale bar 250 μm. Data are representative of three independent experiments.